Short communication

Mechanistic study on lithium intercalation using a restricted reaction field in LiNi$_{0.5}$Mn$_{0.5}$O$_2$

Kazuyuki Sakamoto [a], Hiroaki Konishi [a], Noriyuki Sonoyama [a], Atsuo Yamada [a],
Kazuhisa Tamura [b], Jun'ichiro Mizuki [b], Ryoji Kanno [a,*]

[a] Department of Electronic Chemistry, Interdisciplinary Graduate School of Science and Engineering, Tokyo Institute of Technology,
4259 Nagatuta-cho, Midori-ku, Yokohama 226-8502, Japan
[b] Japan Atomic Energy Agency, Synchrotron Radiation Research Center, Kansai Research Establishment,
1-1-1 Kouto, Sayo-cho, Sayo-gun, Hyogo 679-5148, Japan

Abstract

Structure changes of LiNi$_{0.5}$Mn$_{0.5}$O$_2$ were detected at the electrode/electrolyte interface of lithium cell using synchrotron X-ray scattering and two-dimensional model electrodes. The electrodes were constructed by an epitaxial film of LiNi$_{0.5}$Mn$_{0.5}$O$_2$ synthesized by pulsed laser deposition (PLD) method. The orientation of the film depends on the substrate plane; the 2D layer of LiNi$_{0.5}$Mn$_{0.5}$O$_2$ is parallel to the SrTiO$_3$(1 1 0) substrate ((1 1 0) LiNi$_{0.5}$Mn$_{0.5}$O$_2$//(1 1 0) SrTiO$_3$), while the 2D layer is perpendicular to the SrTiO$_3$(1 1 1) substrate ((0 0 3) LiNi$_{0.5}$Mn$_{0.5}$O$_2$//(1 1 1) SrTiO$_3$). The *in situ* X-ray diffraction of LiNi$_{0.5}$Mn$_{0.5}$O$_2$(0 0 3) confirmed three-dimensional lithium diffusion through the two-dimensional transition meal layers. The intercalation reaction of LiNi$_{0.5}$Mn$_{0.5}$O$_2$ will be discussed.
© 2007 Elsevier B.V. All rights reserved.

Keywords: Epitaxial thin film; Lithium battery; Cathode materials; Intercalation mechanism

1. Introduction

The layered LiMn$_{0.5}$Ni$_{0.5}$O$_2$ is a promising candidate for lithium battery cathode [1–4]. Its crystal structure is a layered rock-salt type (α-NaFeO$_2$ type) composed of alternate layers of lithium and transition metals, both occupying the octahedral space of a cubic close packed anion array [5–7]. The two-dimensional (2D) transition metal layers are formed by edge sharing (Ni,Mn)O$_6$ octahedra, and lithium ions between the subsequent [(Ni,Mn)O$_6$] slab are expected to diffuse in the lithium layer through the interstitial tetrahedral sites. Two orientations of our films make it possible to restrict the surface planes at which the insertion reaction initiates: the (1 1 0) and (0 0 3) orientations correspond respectively to the planes perpendicular and parallel to the edges of 2D-layered structure.

The material is situated in the ternary LiCoO$_2$–LiNiO$_2$–LiMnO$_2$ system, where various compositions were examined to optimize their cathodic properties [8]. For example, LiCo$_{1/3}$Mn$_{1/3}$Ni$_{1/3}$O$_2$ shows high reversible capacities with thermal stabilities of charged state [2,9,10]. However, the capacity decreased with decreasing Co content, and LiMn$_{0.5}$Ni$_{0.5}$O$_2$ showed rather low electrode characteristics. To understand their electrode properties, many structural and mechanistic studies have been reported. For example, local structure ordering has been proposed on the metal layer and lithium diffusion in the metal layer was suggested by first-principal calculation and NMR measurement, which implies three-dimensional lithium diffusion in the two-dimensional-layered material [11,12]. A partial lithium occupation parameters at the tetrahedral site in the lithium layer was also indicated by high flux X-ray diffraction (XRD) measurement, which is consistent with the diffusion of lithium at the metal layer through the tetrahedral site of lithium layer [13]. The isotropic diffusion might be one of the reasons for the irreversible capacity at the first charged process. However, the results indicated previously suggest the unusual diffusion mechanism. We have tried to observe direct evidences of the lithium diffusion in the layered materials.

The epitaxial-film electrodes have advantages for the mechanistic study of lithium (de)intercalation, because the two-dimensional interface restrict their reaction fields; lattice

---

* Corresponding author. Tel.: +81 45 924 5401; fax: +81 45 924 5401.
E-mail address: kanno@echem.titech.ac.jp (R. Kanno).

plane dependence of the reaction might directly be detected [14,15].

In the present study, we synthesized the epitaxial film of the layered $LiMn_{0.5}Ni_{0.5}O_2$ with (0 0 3) and (1 1 0) orientations, and the structure changes during the lithium intercalation were directly observed by *in situ* XRD method for the film of (0 0 3) orientation.

2. Experimental

The epitaxial film of $LiNi_{0.5}Mn_{0.5}O_2$ was synthesized by the PLD method using an apparatus, PLD 3000 (PVD Products Inc.). The films were deposited on the (1 1 0) and (1 1 1) planes of the $SrTiO_3$ substrate (STO: 1 wt% Nb doped) using a KrF excimer laser with a wavelength of 248 nm under O_2. The deposition conditions were as follows: Li/M ratio = 1.3/1; temperature, $T = 600\,^{\circ}C$; distance between substrate and the target, $d = 7.5$ cm; laser frequency, $f = 10$ Hz; deposition time, $t = 180$ min; laser energy, $E = 250$ mJ; and pressure, $pO_2 = 25$ mTorr. The film thickness and roughness of both films determined by X-ray surface reflectometer were about 10 and 0.5 nm, respectively.

Thin films X-ray diffraction data were recorded by a thin film X-ray diffractometer, Rigaku ATX-G apparatus with Cu $K_{\alpha 1}$ radiation. The orientation of the films were characterized both by the out-of-plane and in-plane measurements.

The *in situ* XRD was measured with a κ-type six-circle diffractometer (New Port) installed on a bending-magnet beamline BL14B1 at SPring-8. The X-rays were monochromated by the Si(1 1 1) double crystal system and focused by two Rh-coated bent mirrors. The beam size of the incident X-ray was 0.1 mm (vertical) × 0.4–1.0 mm (horizontal), which was adjusted by a slit placed in front of the sample. The angular acceptance of the receiving slit was 2 mrad for the 2θ direction and 20 mrad for the χ direction. A wavelength of 1.283 Å was selected. The *in situ* spectro-electrochemical cell [14,15] designed for our experiments provided continuous structural changes with the electrochemical lithium intercalation and deintercalation. Electrolyte solution of EC:DEC with 3:7 molar ratio and 1 M $LiPF_6$ was injected into the spectro-electrochemical cell. Intercalation and deintercalation was carried out by the potentiostatic method with a potentiostat/galvanostat (Hokuto Denko, HA-501). The structure changes were observed by the potentiostatic method during the electrochemical (de)intercalation. After the cell potential became constant, the electrolyte was poured out from the outlet of the cell until the Mylar window was placed on the surface of the epitaxial film. This treatment drove all of the N_2 gas, which existed in the cell, out of the cell. This thin layer configuration has advantages in avoiding X-ray scattering by the solution. After the XRD measurements, the electrolyte was poured into the cell again and the potential of the cell was changed to a fixed value for the next measurement. The peak shift was measured for the 0 0 3 and 1 0 4 reflections of the $LiMn_{0.5}Ni_{0.5}O_2$(0 0 3) at an interval of about 0.2 V from the initial voltage of 3.24–5.0 V (versus Li metal) and then from 5.0 to 3.0 V.

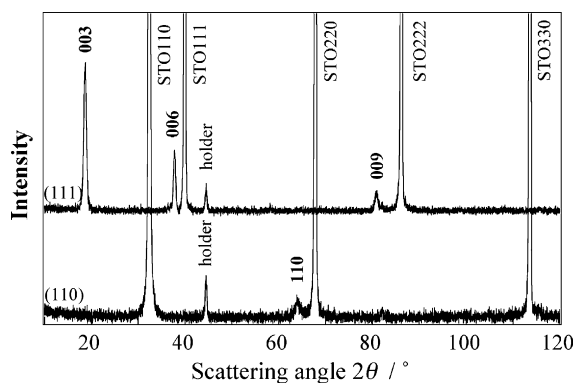Fig. 1. Out-of-plane XRD patterns of $LiNi_{0.5}Mn_{0.5}O_2$ on the STO substrates.

3. Results and discussion

3.1. Characterization of the epitaxial films

Fig. 1 shows the XRD patterns of the out-of-plane measurements for $LiMn_{0.5}Ni_{0.5}O_2$ films on the different substrate planes, STO(1 1 0) and (1 1 1). The patterns indicate the orientation normal to the substrate plane. The $LiMn_{0.5}Ni_{0.5}O_2$ film on the STO(1 1 0) plane showed the reflections near 64° which was indexed as 1 1 0 based on the hexagonal lattice. The film on the STO(1 1 1) plane showed the reflections near 19°, 38°, and 80° which were indexed as 0 0 3, 0 0 6, and 0 0 9 based on the hexagonal lattice. These films have the (1 1 0) and (0 0 3) orientations on (1 1 0) and (1 1 1) substrates, respectively.

The in-plane XRD was measured along [1, −1, 1] and [1, −1, 0] for STO(1 1 0) and (1 1 1) planes of the substrates, respectively (see Fig. 2). The in-plane measurement along [1, −1, 1] of the substrate indicated 0 0 l reflections of $LiMn_{0.5}Ni_{0.5}O_2$ on the STO(1 1 0) substrate. The 1 1 0 reflection of $LiMn_{0.5}Ni_{0.5}O_2$ was observed for the in-plane measurement along [1, −1, 0] of the STO(1 1 1) substrate. Figs. 3 and 4 show the φ-scan XRD patterns of 0 0 6 and 1 1 0 reflections of $LiMn_{0.5}Ni_{0.5}O_2$ in the substrate plane. Four peaks were observed at intervals of 70° and 110° for 0 0 6 reflection of $LiMn_{0.5}Ni_{0.5}O_2$(1 1 0), indicating twin structure for the (1 1 0) orientation. The six-fold symmetry observed for 1 1 0 reflection of $LiMn_{0.5}Ni_{0.5}O_2$(0 0 3), which is consistent with the hexagonal lattice. These results indicate the epitaxial films of $LiMn_{0.5}Ni_{0.5}O_2$ with different lattice
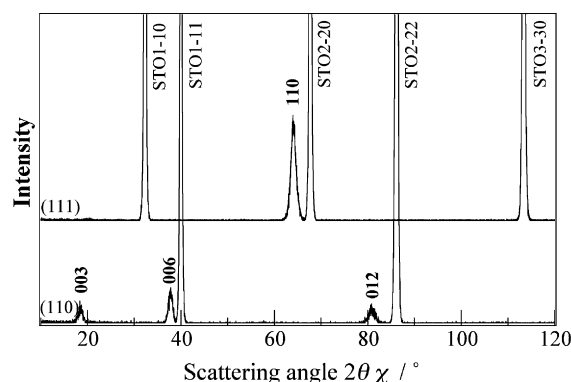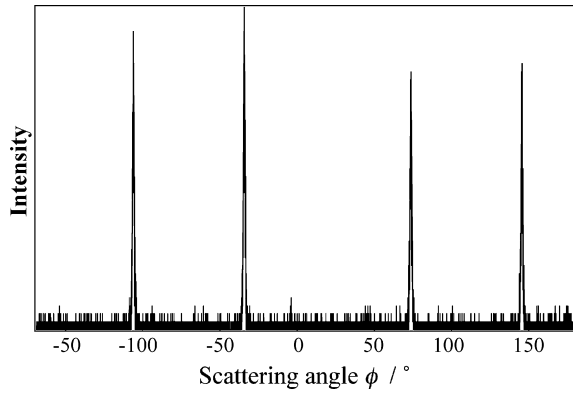

Fig. 2. In-plane XRD patterns of $LiNi_{0.5}Mn_{0.5}O_2$ on the STO substrates.

Fig. 3. XRD patterns of in-plane ϕ-scan for LiMn$_{0.5}$Ni$_{0.5}$O$_2$ on the STO(1 1 0).

Fig. 4. XRD patterns of in-plane ϕ-scan for LiMn$_{0.5}$Ni$_{0.5}$O$_2$ on the STO(1 1 1).

orientations on the SrTiO$_3$ substrates. The relationship between the LiMn$_{0.5}$Ni$_{0.5}$O$_2$ and the STO substrate orientations is summarized in Table 1, together with their schematic drawing of the 2D structure.
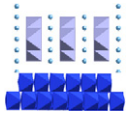
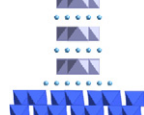### 3.2. In situ XRD measurements of the thin film electrodes

The 0 0 3 and 1 0 4 peaks of the LiNi$_{0.5}$Mn$_{0.5}$O$_2$(0 0 3) film electrode are shown in Figs. 5 and 6, respectively. The 0 0 3 peak shifts to lower d-values with anodic polarization from the initial
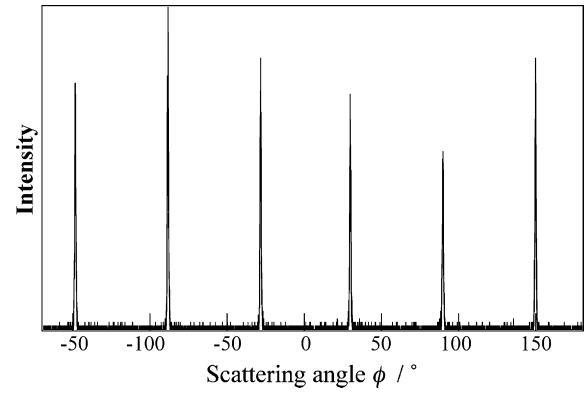
voltage of 3.24 V. The peak shifts again to the opposite direction, higher d-values, with cathodic polarization. As the (0 0 3) plane is parallel to the two-dimensional transition metal layers, no 2D edges exist at the surface of the electrode. However, the peak shift of 0 0 3 indicated the lithium (de)intercalation through the surface of (0 0 3) with applying voltages. On the other hand, the 1 0 4 peak shifts to lower d-values with anodic polarization from the initial voltage of 3.24 V, while the peak remains almost constant with the cathodic polarization. The lattice parameters were thus calculated from the d-values of 0 0 3

Table 1
Relationship between the substrate orientation and the out-of-plane and in-plane lattice orientation of the LiN$_{0.5}$Mn$_{0.5}$O$_2$

	LiNi$_{0.5}$Mn$_{0.5}$O$_2$(1 1 0) on SrTiO$_3$(1 1 0)	LiNi$_{0.5}$Mn$_{0.5}$O$_2$(0 0 3) on SrTiO$_3$(1 1 1)
Out-of-plane	LiNi$_{0.5}$Mn$_{0.5}$O$_2$(1 1 0)//SrTiO$_3$(1 1 0)	LiNi$_{0.5}$Mn$_{0.5}$O$_2$(0 0 3)//SrTiO3(111)
In-plane	LiNi$_{0.5}$Mn$_{0.5}$O$_2$[0 0 1]//SrTiO$_3$[1, −1, 1]	LiNi$_{0.5}$Mn$_{0.5}$O$_2$[1 1 0]//SrTiO$_3$[1, −1, 0]
Structure		
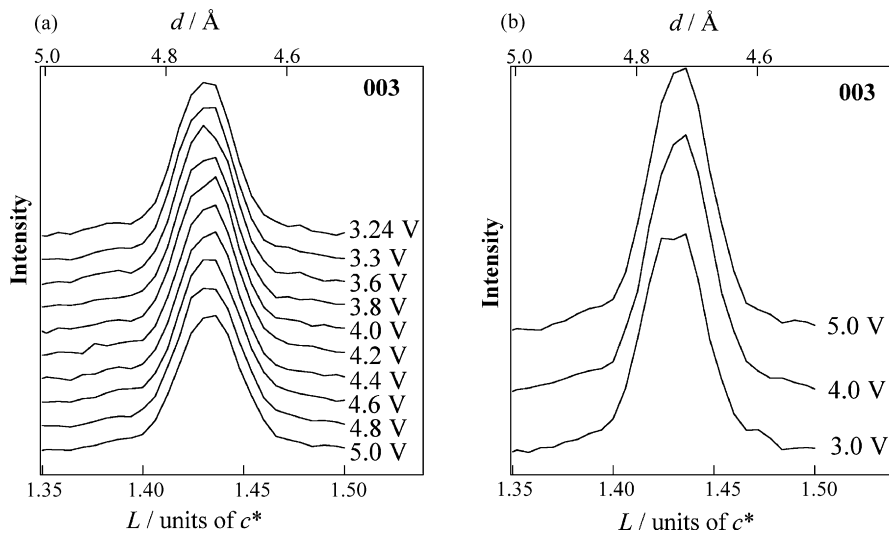
Fig. 5. In situ XRD patterns of the 0 0 3 reflection for the LiNi$_{0.5}$Mn$_{0.5}$O$_2$(0 0 3) deposited on the STO(1 1 1). The 0 0 3 reflection of LiNi$_{0.5}$Mn$_{0.5}$O$_2$(0 0 3) was measured along the [0 0 l] directions of the STO(1 1 1). The data are plotted as a function of the reciprocal lattice of the STO(1 1 1), l, and the d-value for LiNi$_{0.5}$Mn$_{0.5}$O$_2$(0 0 3). The peak shifts during the anodic polarization from the initial voltage to 5.0 V (a) and the shift during the cathodic polarization to 3.0 V (b).
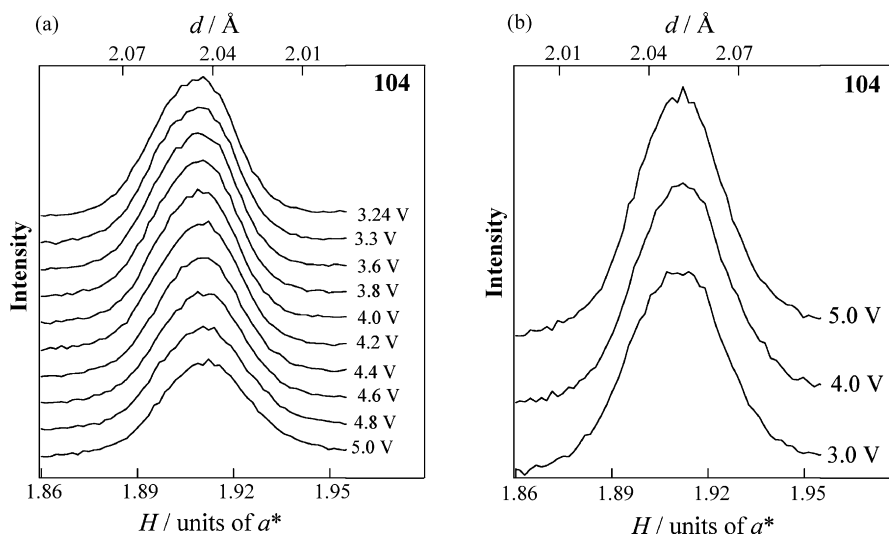
Fig. 6. *In situ* XRD patterns for the $LiNi_{0.5}Mn_{0.5}O_2(0\,0\,3)$ deposited on the STO(1 1 1). The 1 0 4 reflection of $LiNi_{0.5}Mn_{0.5}O_2(0\,0\,3)$ was measured along the [$h\,0\,h$] directions of the STO(1 1 1). The data are plotted as a function of the reciprocal lattice of the $SrTiO_3$ substrate, h, and the d-value for $LiNi_{0.5}Mn_{0.5}O_2(0\,0\,3)$. The peak shifts during the anodic polarization from the initial voltage to 5.0 V (a) and the shift during the cathodic polarization to 3.0 V (b). Our direct structure observation during the electrochemical reaction.

and 1 0 4 peaks. Fig. 7 summarizes the applied potential dependence of the lattice parameter of the $LiNi_{0.5}Mn_{0.5}O_2(0\,0\,3)$. The lattice parameter, c, decreases with increasing voltage from 3.24 to 5.0 V, corresponding lithium deintercalation. The parameter increased again with decreasing voltages from 5.0 to 3.0 V due to the reverse reaction. On the other hand, the lattice parameter, a, decreased with increasing voltage from 3.24 to 5.0 V, with no increase in parameter during the reverse process from 5.0 to 3.0 V. These results indicate that lithium deintercalates from both the Li and TM (transition metal; Ni, Mn) layers and diffuses three dimensionally in the 2D structure with applying voltage from 3.24 to 5.0 V (charge). During the reverse reaction, the increase in the c parameter indicated that lithium penetrates 2D $[(Ni,Mn)O_6]_\infty$ layer from the (0 0 3) surface, and diffuses three dimensionally in the 2D structure. No significant change in the a parameter suggests that lithium inserted into the Li layer without occupying again the TM layer. About 8–12% of cation exchange (Li and Ni) was reported between the Li and TM layers [1–4]. Three-dimensional diffusion might be explained by the lithium passing through the Li sites in the
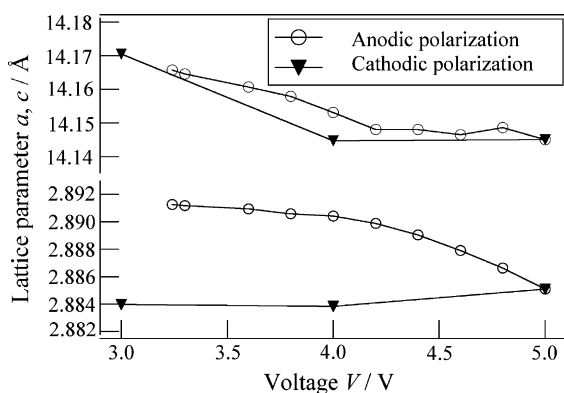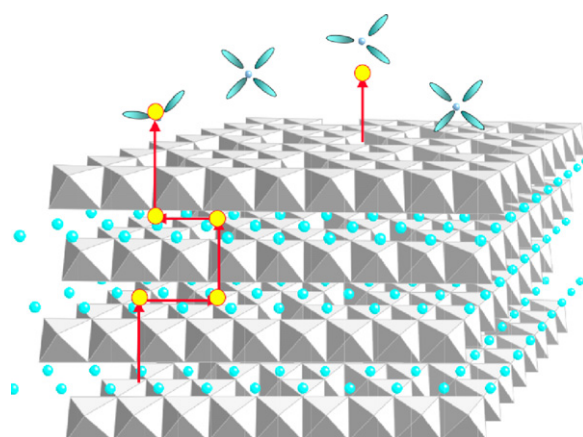

Fig. 8. Schematic drawing of the $LiMn_{0.5}Ni_{0.5}O_2(0\,0\,3)$ film. The (0 0 3) plane is parallel to the two-dimensional edges of the layered structure. The deintercalation of lithium form the Li-layer and TM layer proceeded from 3.24 to 5.0 V.

TM layer, which is consistent with the previous reports indicating lithium diffusion through the TM layer [11–13]. Our direct structure observation during the electrochemical reaction clarified the three-dimensional diffusion on the 2D-layered material (see Fig. 8).

4. Summary

We observed the bulk structure changes during the electrochemical reactions for $LiNi_{0.5}Mn_{0.5}O_2$. The $LiNi_{0.5}Mn_{0.5}O_2$ films have the 2D transition metal layer parallel and perpendicular to the substrates depending on the substrate orientation. Direct observation of lithium (de)intercalate process using *in situ* XRD measurements suggests that the lithium deintercalates through the Li and TM layers at the first charge process, which indicates three-dimensional lithium diffusion in the 2D layer structure. However, irreversible lattice parameter changes

Fig. 7. The voltage vs. lattice parameter curves for $LiNi_{0.5}Mn_{0.5}O_2(0\,0\,3)$ deposited on the STO(1 1 1).

observed for the discharge process suggests that lithium inter-calate into the Li layer without occupying the TM layer. The mechanistic study using a restricted lattice plane are unique and efficient technique to clarify the (de)intercalation mechanism for lithium battery electrodes.

Acknowledgements

References

[1] T. Ohozku, Y. Makimura, Chem. Lett. 8 (2001) 744.

[2] Z.H. Lu, D.D. MacNeil, J.R. Dahn, Electrochem. Solid-State Lett. 4 (2001) A191.
[3] Y. Makimura, T. Ohzuku, J. Power Sources 119–121 (2003) 156.
[4] C. Delmas, et al., J. Power Sources 68 (1997) 120.
[5] L. Croguennec, C. Pouillerie, A.N. Mansour, C. Delmas, J. Mater. Chem. 11 (1) (2001) 131–141.
[6] R.K.B. Gover, R. Kanno, B.J. Mitchell, M. Yonemura, Y. Kawamoto, J. Electrochem. Soc. 147 (2000) 4045–4051.
[7] I. Saadoune, C. Delmas, J. Solid State Chem. 136 (1) (1998) 8–15.
[8] Y. Koyama, et al., J. Electrochem. Soc. 151 (9) (2004) A1499.
[9] T. Ohzuku, Y. Makimura, Chem. Lett. 30 (2001) 744.
[10] Z.H. Lu, L.Y. Beaulieu, R.A. Donaberger, C.L. Thomas, J.R. Dahn, J. Electrochem. Soc. 149 (2002) A778.
[11] A. Van der Ven, G. Ceder, Electrochem. Commun. 6 (2004) 1045.
[12] C.P. Grey, W.S. Yoon, J. Reed, G. Ceder, Electrochem. Solid-State Lett. 7 (2004) A290.
[13] H. Kobayashi, Y. Arachi, H. Kageyama, K. Tatsumi, J. Mater. Chem. 14 (2004) 40.
[14] K. Sakamoto, M. Hirayama, T. Hiraide, D. Mori, A. Yamada, R. Kanno, K. Tamura, J. Mizuki, in preparation.
[15] M. Hirayama, K. Sakamoto, T. Hiraide, D. Mori, A. Yamada, R. Kanno, K. Tamura, J. Mizuki, Electrochimica Acta, in press.